CORRECTING FOR DISTORTED ANTENNA PATTERNS IN CODAR OCEAN SURFACE MEASUREMENTS

DONALD E. BARRICK and BELINDA J. LIPA

Reprinted from IEEE Journal of Oceanic Engineering, Vol. OE-11, No. 2, April 1986

Correcting for Distorted Antenna Patterns in CODAR Ocean Surface Measurements

DONALD E. BARRICK, MEMBER, IEEE, AND BELINDA J. LIPA

(*Invited Communication*)

Abstract—**CODAR systems employ compact antenna elements such as electrically small loops and monopoles to extract bearing information in ocean surface observations. Past analysis methods have assumed that these element patterns are perfect, i.e., cosine and omnidirectional. Operations from metallic offshore platforms usually distort these patterns because of unavoidable objects in their near field. When such distortions are ignored, previous methods are shown to produce ~35° rms bearing errors. Therefore least-squares methods are presented and demonstrated that deal with differential element pattern distortions. It is shown how the required relative patterns are easily measured by a boat circling the antenna, and these patterns are then stored as look-up tables in the least-squares inversion methods. Relative patterns (i.e., one element pattern divided by the other), rather than absolute, are all that are required for extraction of surface current, wave-height directional spectra, wind direction, and drifting transponder information with CODAR.**

I. Introduction

THE CODAR concept embodies all HF radar systems for measurement of ocean surface currents, waves, ice, surface winds, and transponding drifters that employ compact antenna systems. This concept contrasts with the much larger phased-array antennas that are required when a narrow radar beam (in azimuth) is to be formed and scanned. CODAR's can be sited either on the coast, on islands, or on offshore platforms such as oil rigs. The types of antenna systems that have been employed with CODAR include: 1) three- or four-element quarter-wave monopole receiving arrays (with interelement spacings between $\lambda/3$ and $\lambda/2$, where λ is the radar wavelength), with the coverage area illuminated by a separate broad-beamed transmitting antenna [1], [2]; and 2) a three-element crossed-loop/monopole structure [3], [4] that is less than $\lambda/4$ in height and $\lambda/10$ in lateral dimension. The monopole element of 2) is used for transmission, rather than a separate antenna as required in 1). The latter CODAR antenna has been the only system compact enough for use on offshore towers at the normal operating frequencies of 25 MHz, where radar wavelength is 12 m.

The three/four-element monopole receive arrays, as they have been used in the past, determine direction of arrival of the signal(s) at a given Doppler frequency from various closed-form mathematical equations in terms of the complex voltage cross spectra at each of the antenna elements [1], [2]. From these solutions, estimates of radial current velocity versus range and bearing are constructed. Assumed in the use of these closed-form solutions are: a) perfect omnidirectional patterns for each of the monopole antenna elements, and b) no noise added to the received sea-echo signal voltages. In [5] it is shown that mutual interaction among the four elements, neglected in the closed-form solutions, will produce sufficient pattern distortion to cause bearing biases with this system. Although mutual interaction among elements is not a problem with the crossed-loop system [3], [4], recent operations from offshore platforms have shown that the metallic structure beneath and around the antenna can significantly distort the patterns of the three elements. Hence the assumption that the loops have cosine patterns and the monopole has an omnidirectional pattern in the least-squares [3] analysis methods used to extract directional information may not be valid. Furthermore, it is not generally possible to remove *all* pattern distortion by physically moving the antenna to the highest point on the tower (even when the monopole is fed against horizontal radial wires), for any unsymmetric metal structure in the near field below the antenna will distort the element patterns.

This paper shows how to employ the actual distorted patterns in the analysis of directional data received by CODAR. It is necessary only to measure the three-element patterns with the antenna structure in place; from an offshore platform, this is easily done with one pass of a boat in a circle around the platform, carrying a signal source or transponder. The measured patterns are then stored in arrays in the inversion software, and applied in the data analysis; the methods are presented and demonstrated for surface currents. The unique nature of the sea echo and the least-squares formulation makes it unnecessary to know the *absolute* patterns of the three elements. Only the *relative* patterns between them need be known—a much simpler quantity to deal with.

As an introductory illustration of the severity of unsymmetrically placed metal around the CODAR antenna system, we calculate here the loop and monopole patterns for the structure shown in Fig. 1(a). One electrically small loop with a monopole through its vertical plane simulates the CODAR situation. (The other orthogonal loop is omitted here since its pattern is inferred from the first by symmetry.) In the absence of any distortion, and with the patterns normalized to unity at the loop maxima, the solid circle and cosine curve show the

Manuscript received August 23, 1985; revised January 22, 1986.
D. E. Barrick is with Ocean Surface Research, Boulder, CO 80303.
B. J. Lipa is with Ocean Surface Research, Woodside, CA 94062.
IEEE Log Number 8608304.

0364-9059/86/0400-0304$01.00

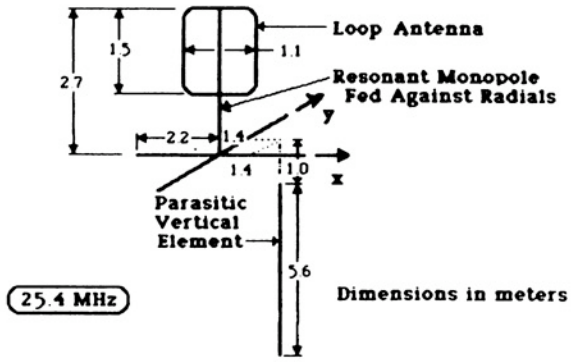

(a)

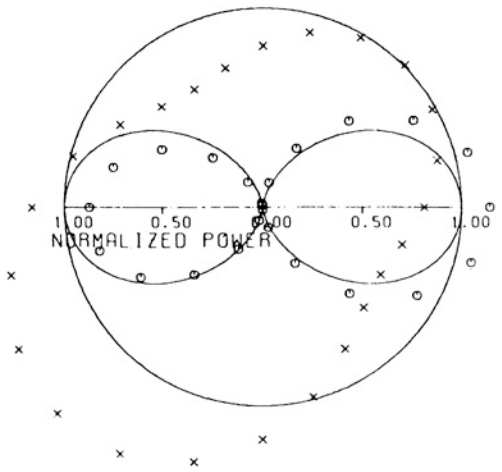

(b)

Fig. 1. (a) Loop-monopole structure with four radial elements at 25.4 MHz, with off-center parasitic rod below used to model pattern distortion with MININEC. (b) Patterns of loop and monopole *without* rod present (solid curves) and distorted patterns caused by rod (circles are loop pattern and crosses are monopole pattern). Both are power patterns, i.e., $|A_1(\varphi)|^2$ and $|A_3(\varphi)|^2$.

perfect desired patterns. We then introduce an isolated vertical element 1-m below the radial wires, off center from the axis of symmetry by 1.4 m from each orthogonal radial axis (i.e., ~2 m from center), as shown in the figure. At 5.6 m in length, the vertical element is essentially a dipole at nearly $\lambda/2$ resonance, a "worst-case" situation. The dotted points show the resulting loop and monopole patterns produced by this parasitic unsymmetrical element in the near field. These patterns were calculated using MININEC, one of the widely available highly accurate moment-method codes [6] for computing currents induced on wire structures with excitations at any position; from these currents, far-field patterns are calculated for vertical polarization. The monopole pattern is seen to suffer somewhat greater distortion than the loop by such near-field obstacles. This example is meant only to illustrate how severely ideal patterns can be distorted by nearby metallic objects. Use of perfect patterns in inversion methods when the actual patterns are distorted as shown will clearly result in significant biases in derived sea-surface information. The magnitude of this error will be illustrated subsequently using a pattern measured from a rig on which CODAR operates, and simulating extracted angles by incorrectly assuming perfect patterns.

II. Voltages Received at Antennas

A. Perfect Crossed-Loop/Monopole Patterns

As in [3], we can write expressions for the complex received signal voltages of the two electrically small crossed-loop (designated with subscripts 1 and 2) and monopole (subscript 3) antenna elements when their patterns are perfect. These voltages are implicitly a function of Doppler (spectral) frequency, i.e., the time signal has been Fourier transformed for a given range cell, so that at a given spectral frequency ω these signal voltages are

$$V_1 = (1/2\pi) \int_{-\pi}^{\pi} \cos\ \varphi g(\varphi)\ d\varphi \tag{1a}$$

$$V_2 = (1/2\pi) \int_{-\pi}^{\pi} \sin\ \varphi g(\varphi)\ d\varphi \tag{1b}$$

$$V_3 = (1/2\pi) \int_{-\pi}^{\pi} g(\varphi)\ d\varphi \tag{1c}$$

where φ is the bearing angle from the Loop 1 axis to the signal return, and $g(\varphi)$ is a complex function that describes the distribution of signal strength arriving from bearing φ. Hence, the integral represents a summation of signals versus their angles of arrival, weighted by the antenna patterns. Since the patterns are assumed perfect, we also take the amplitude and phase factors among them to be adjusted so that the loop and monopole strengths are equal at the positive lobes of each loop. For the sake of illustration here, we assume we are operating from a platform so that signals can arrive from 360° of space, i.e., $-\pi < \varphi < \pi$, although this is not necessary in general (see [3]). If $g(\varphi)$ represents sea echo distributed continuously over space, then it is a Gaussian random variable uncorrelated at different bearings, i.e.,

$$\sigma'(\omega,\ \varphi)\delta(\varphi - \varphi') = \langle g(\varphi) g^*(\varphi') \rangle / 2\pi \tag{2}$$

where angular braces indicate infinite ensemble average, $\delta(x)$ is the Dirac delta function of argument x, * denotes complex conjugate, and $\sigma'(\omega, \varphi)$ is referred to as the narrow-beam (power) pattern of the sea echo. If the received signal source, on the other hand, is a single signal arriving from direction φ_0, then $g(\varphi)$ can be written as $A\,\delta(\varphi - \varphi_0)$, where A is a complex constant representing the signal intensity.

B. Arbitrary or Distorted Antenna Patterns

Assume now that the three crossed-loop/monopole elements no longer have the idealized cos φ, sin φ, and 1 patterns used in (1). Take their element patterns instead to be $A_1(\varphi)$, $A_2(\varphi)$, and $A_3(\varphi)$, where these response patterns are in general complex. In keeping with the operation of the CODAR crossed-loop system, we assume that the signal is transmitted through the monopole (Element 3), while reception takes place through each of the three elements sequentially. Hence, for sea echo (or any linear signal propagation-scatter process), the received signal is weighted by both the transmit and receive patterns. The equations analogous to (1) are

$$V_1 = (1/2\pi) \int_{-\pi}^{\pi} A_1(\varphi) A_3(\varphi) g(\varphi)\ d\varphi \tag{3a}$$

$$V_2 = (1/2\pi) \int_{-\pi}^{\pi} A_2(\varphi) A_3(\varphi) g(\varphi)\ d\varphi \tag{3b}$$

$$V_3 = (1/2\pi) \int_{-\pi}^{\pi} A_3(\varphi) A_3(\varphi) g(\varphi)\ d\varphi. \tag{3c}$$

We now define and employ here "relative patterns," i.e., the patterns of the loops (Elements 1 and 2) normalized to the monopole pattern (Element 3); we also define a new signal angular distribution $g'(\varphi)$ absorbing Element 3 pattern into it:

$$a_1(\varphi) \equiv A_1(\varphi)/A_3(\varphi)$$

$$a_2(\varphi) \equiv A_2(\varphi)/A_3(\varphi)$$

$$a_3(\varphi) \equiv A_3(\varphi)/A_3(\varphi) = 1$$

and

$$g'(\varphi) \equiv A_3^2(\varphi) g(\varphi). \tag{4}$$

This is done for three reasons: 1) it is extremely difficult to measure absolute antenna patterns after installation at an operational location such as an offshore rig, because the signal arriving from the boat always contains unknown amplitude and phase fluctuations due to source output drifts, boat motion, boat radial position uncertainties, and boat aspect variations; 2) for current and wave measurement, it is *not* necessary to know $g(\varphi)$ or $\sigma'(\omega, \varphi)$, and hence absorbing an unknown absolute pattern $A_3(\varphi)$ into it does not affect subsequent calculations; and 3) far-field obstructions to the antenna system (the more likely occurrence after installation) will distort all three patterns in the same way, and hence this normalization will automatically remove such distortion from the relative patterns that are used. With this new normalization, the received voltages can now be written as

$$V_1 = (1/2\pi) \int_{-\pi}^{\pi} a_1(\varphi) g'(\varphi)\ d\varphi \tag{5a}$$

$$V_2 = (1/2\pi) \int_{-\pi}^{\pi} a_2(\varphi) g'(\varphi)\ d\varphi \tag{5b}$$

$$V_3 = (1/2\pi) \int_{-\pi}^{\pi} g'(\varphi)\ d\varphi. \tag{5c}$$

C. Boat Measurement of Antenna Patterns

It is relatively simple to measure the CODAR antenna patterns after installation by carrying a transponder or stable signal source aboard a boat. The boat circles the platform or coastal site (for coastal operation, only the pattern over the ocean is relevant) at a visible distance (e.g., a few hundred meters); its range and absolute signal emission level are not important in the relative pattern measurement needed here. We have measured such patterns both with the boat circling at constant speed, where $\varphi_b = v_b t$, or where the boat stops at N fixed locations φ_{bi}, $i = 1, \cdots, N$. In both cases, the positions of the boat must be measured so that its location can later be correlated with the CODAR received signals. The CODAR system is programmed to receive and record data in the normal fashion, alternating reception of signals among the three antenna elements every 0.5 ms. Then the signal received from the boat can be written as

$$g(\varphi) = F(\varphi)\delta(\varphi - \varphi_b) \tag{6}$$

and when substituted into (3) will give

$$V_1 = (1/2\pi) A_1(\varphi_b) A_3(\varphi_b) F(\varphi_b) \tag{7a}$$

$$V_2 = (1/2\pi) A_2(\varphi_b) A_3(\varphi_b) F(\varphi_b) \tag{7b}$$

$$V_3 = (1/2\pi) A_3(\varphi_b) A_3(\varphi_b) F(\varphi_b) \tag{7c}$$

where $F(\varphi_b)$ is the signal emitted by the boat.

Hence, the desired relative patterns are obtained by division of the complex voltages

$$a_1(\varphi_b) = V_1/V_3$$

$$a_2(\varphi_b) = V_2/V_3. \tag{8}$$

This process can be done either in the time domain or the frequency domain. If the received time-series signals are Fourier transformed to the frequency domain, the sideband peak representing the boat signal is located in the three antenna spectra, and the complex voltages at a given frequency in this peak are the V_1, V_2, and V_3 used in the above process.

The relative patterns can also be obtained in the time domain, without resort to spectral analysis, if one ascertains that the boat signal received is much stronger than received sea echo and noise. Then one forms the averages across the time-series segment t_m, $1 < m < M$, of voltage cross-product terms, i.e.,

$$\langle V_i V_j^* \rangle = (1/M) \sum_{m=1}^{M} v_i(t_m) v_j^*(t_m) \tag{9}$$

where $v_i(t_m)$ is the complex time-series voltage for antenna "i" at time t_m composed of the in-phase (real) and quadrature (imaginary) channels of the digitized receiver output. The normalized antenna patterns for this time-series segment with the boat at bearing φ_b can now be obtained as

$$a_1(\varphi_b) = \langle V_1 V_3^* \rangle / \langle V_3 V_3^* \rangle$$

and

$$a_2(\varphi_b) = \langle V_2 V_3^* \rangle / \langle V_3 V_3^* \rangle. \tag{10}$$

III. Use with Cross Spectra in Least-Squares Formulation

A. Arbitrary or Distorted Patterns

In the process of extracting surface information from CODAR signals, some form of the received voltages is related to models that are known physically to describe the scattered signal spectrum. The models are posed in terms of unknown parameters, to be determined in this process. When the data contain noise and errors, the optimum technique for extracting these parameters is maximum likelihood, which reduces to least squares because the signals are Gaussian [3]. We have found over many years that the most useful form for the

received signals for such least-squares inversion methods consists of averaged cross spectra among the three antenna voltages. The average of N samples at a given Doppler frequency ω is a generalized chi-squared random variable with $2N$ degrees of freedom [3], from which covariances among the cross spectra are easily constructed for subsequent use in optimal parameter extraction and uncertainty estimation. (In fact, even the older closed-form methods for extracting bearing angles for current estimation use cross spectra [1], [7], [8].)

Hence, let us define $C_{ij} \equiv \langle V_i V_j^* \rangle$ as the average voltage cross spectrum at frequency ω from antennas "i" and "j". In the strict sense, the angular braces denote infinite ensemble averages; when we are dealing with data, we will understand them to mean N-sample averaged quantities. Then the maximum likelihood process for extraction of information from the data (e.g., current, wavefield, transponder parameters) can be posed as a least-squares quadratic form involving premultiplication and postmultiplication of a square matrix by row and column vectors

$$[C_{ij}^D - C_{ij}^M]^T [C_{ij}^{kl}]^{-1} [C_{kl}^D - C_{kl}^M] \Rightarrow \text{minimum} \qquad (11)$$

where superscripts D and M denote data and model, T denotes transpose, -1 is matrix inverse, and for strict maximum likelihood interpretation, C_{ij}^{kl} are the covariance matrix elements among the i, j and k, l cross spectra.

The model cross-spectral elements to be used in (11) above are defined in terms of the relative antenna patterns and the signal's angular power distribution from (2) and (3) as

$$C_{ij}^M(\omega) \equiv P_{ij} + jQ_{ij} = (1/2\pi) \int_{-\pi}^{\pi} a_i(\varphi) a_j^*(\varphi) \sigma'(\omega, \varphi)\, d\varphi. \qquad (12)$$

The model $\sigma'(\omega, \varphi)$ will contain the first-order solution for HF sea scatter if ω is chosen to lie within the Bragg-peak region of the echo spectrum, or the second-order solution if ω lies elsewhere; or ω could define the location of a transponder sideband. The first case is used for current extraction, the second for wave-height directional information extraction, and the third for drifter/transponder location and tracking. In all of these cases, the model σ' contains unknown parameters to be determined by minimizing the above least-squares sum. The relative pattern products $a_i(\varphi) a_j^*(\varphi)$ are now assumed known from boat measurements, and stored as look-up tables for use in the least-squares fitting process.

B. Application to Surface Current Extraction

We demonstrate use of the above method for the extraction of surface currents with CODAR. In this case, the first-order echo signal σ' reduces to Dirac-delta functions involving the radial velocity (directly proportional to Doppler shift ω) as a function of unknown angle φ at $m < M$ discrete positions [3, eq. (27)]. For the dual-angle case ($M = 2$), for example, the delta-function constraints reduce the integral model (12) to

$$C_{ij}^M = p_1 a_i(\varphi_1) a_j^*(\varphi_1) + p_2 a_i(\varphi_2) a_j^*(\varphi_2) \qquad (13)$$

where the four unknown parameters in the model to be determined by least-squares fitting are p_1, p_2, φ_1, and φ_2. Two of these, p_1 and p_2, appear as linear factors, and are easily removed. The two unknown angles, φ_1 and φ_2, are found by a grid search for the minimum in a straightforward manner [3]. Finally, we employ the identity matrix for C_{ij}^{kl} in this implementation of least squares because the covariance matrix is singular in the first-order region [3].

We illustrated the application to measured data for CODAR operations in the spring of 1984 aboard the Treasure SAGA (a semi-submersible offshore oil rig in the North Sea). The crossed-loop/monopole antenna system was mounted on top of the derrick at the center of the rig. There were many metallic objects such as anemometers and lights that were unavoidably arrayed in an unsymmetric fashion within 2 m of the antenna system and its radial counterpoise. At an operating frequency of 25.4 MHz (wavelength of ~ 12 m), these obstacles were clearly in the near field of the antenna. Using the method described earlier, we measured the distorted patterns with a boat circling the rig, and employed these patterns to extract surface currents with least squares, based on (11) and (13) above. Fig. 2 shows the distorted normalized power patterns we measured ($|a_1(\varphi)|^2$ and $|a_2(\varphi)|^2$) as the solid curves. Note that if these patterns were perfect, they would be $\cos^2 \varphi$ and $\sin^2 \varphi$. Plotted are two examples of the radial current vector maps recovered based on these techniques. Analyses and simulations show that the gaps seen in certain sectors are caused by the nonnegligible motion of the floating rig in response to waves. Radial vector maps such as these are the basic output of a single CODAR station when measuring currents. Such radial maps can be interpreted in any number of ways to obtain circulation information (e.g., combination with data from another station to produce total vectors, use of models to estimate total vectors from single site data, etc.), as described in [3].

C. Relationship to Previous Methods for Perfect Patterns

Although the present approach appears different from that detailed in [3] for perfect crossed-loop/monopole patterns, the differences are minor. Advantage was taken in [3] of the fact that the perfect $\cos \varphi$, $\sin \varphi$, and 1 antenna element patterns were also coincidentally the first three basis functions of the angular Fourier series. Hence, all angular wave and echo pattern fields were expanded in these trigonometric basis functions, and a broad-beam pattern could be written in terms of the narrow-beam pattern $\sigma'(\omega, \varphi)$ as

$$\sigma(\omega, \psi) = (1/2\pi) \int_{-\pi}^{\pi} \cos^4 [(\psi - \varphi)/2] \sigma'(\omega, \varphi)\, d\varphi \qquad (14)$$

$$\equiv (1/2\pi) \sum_{n=-2}^{2} b_n(\omega) tf_n(\psi) \qquad (15)$$

where $tf_n(\psi)$ are the trigonometric basis functions defined by

$$tf_n(\psi) \equiv \begin{cases} \cos(n\psi), & \text{for } n \geq 0 \\ \sin|n\psi|, & \text{for } n < 0. \end{cases} \qquad (16)$$

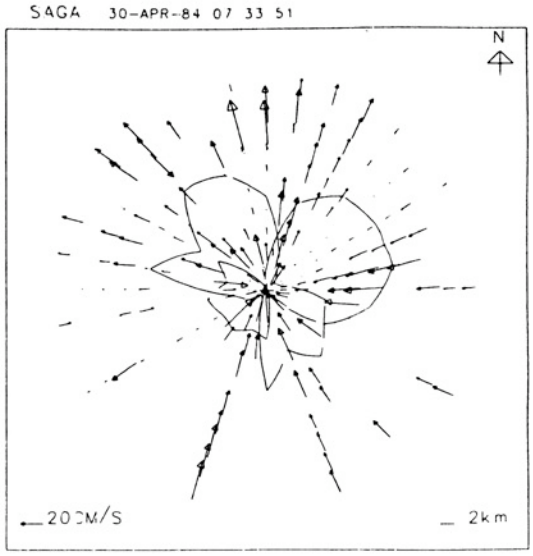

(a)

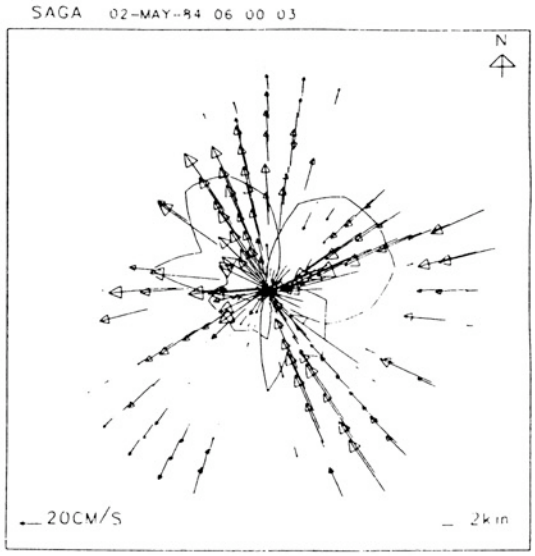

(b)

Fig. 2. Normalized relative CODAR antenna patterns $|a_1(\varphi)|^2$ and $|a_2(\varphi)|^2$ measured on offshore oil rig "Treasure SAGA" (solid curves), to be compared with $\cos^2\varphi$ and $\sin^2\varphi$ perfect patterns. Vectors are examples of radial current velocities around the rig recovered using methods presented here for the distorted patterns shown.

With these definitions, then, the data signals measured from the three antennas were expressed in terms of cross spectra related to the $b_n(\omega)$ as

$$b^D_{-2}(\omega) = 2\pi\langle \mathrm{Re}\ [V_1 V_2^*]\rangle$$

$$b^D_{-1}(\omega) = 4\pi\langle \mathrm{Re}\ [V_2 V_3^*]\rangle$$

$$b^D_0(\omega) = 3\pi\langle |V_3|^3\rangle$$

$$b^D_1(\omega) = 2\pi\langle \mathrm{Re}\ [V_1 V_3^*]\rangle$$

$$b^D_2(\omega) = \pi\langle |V_1|^2 - |V_2|^2\rangle \qquad (17)$$

and the model counterparts to (12) and (13) are

$$b^M_n(\omega) = q_n \int_{-\pi}^{\pi} \sigma'(\omega, \varphi) t f_n(\varphi)\, d\varphi$$

$$= q_n[p_1 t f_n(\varphi) + p_2 t f_n(\varphi)] \qquad (18)$$

where $q_{\pm 2} = 1/8$, $q_{\pm 1} = 1/2$, and $q_0 = 3/8$. Then the least-squares minimization with the identity weight matrix C^{kl}_{ij} reduces to

$$\sum_{n=-2}^{2} [b^D_n - b^M_n]^2 \Rightarrow \text{minimum.} \qquad (19)$$

Hence, in both cases, the problem is posed in terms of cross spectra among the antenna element voltages. In the case of perfect patterns for a given Doppler frequency ω, there are five cross-spectral data values that appear in (19) above, while in principle there are nine real co- and quad-spectral data values that are available for use in (11). This happens because *all* of the quad-spectra (imaginary parts of the cross spectra) are zero when the antenna patterns are perfect. Furthermore, there is an identity relationship among the six co-spectra, reducing their number to five. When the three antenna patterns are arbitrary and in general complex, however, there is no obvious way to reduce their number. Whether this implies that it is possible to extract more information (e.g., nine unknown constants) from the least-squares process when the patterns are more complex than the simple cos φ, sin φ, and 1 is not known at this point, and has not been tested. It is certain that *at least* as much information on currents and waves is available when the patterns are more general.

D. Simulations of Error in Neglect of Distorted Antenna Patterns

The question that is relevant is how much error in output is encountered when the element patterns are distorted but extraction methods assuming perfect patterns are employed? To obtain a quantitative feeling for this error, we used the actual distorted patterns measured at Treasure SAGA and shown in Fig. 2 with simulations. Simulations were selected for this error study over actual measured sea echo because we know the precise input, or "truth," with the former. CODAR observations of currents flowing past a platform will encounter signals arriving from two directions, φ_1 and φ_2, at each Doppler frequency ω. Therefore we employed the model given by (13) for two signals to generate cross spectra, using the actual distorted normalized patterns $a_i(\varphi)$ $(i = 1, 2)$. With these cross spectra, we then calculated the five b^D_n as required in (17) above for perfect patterns, and used the model of (18) and the least-squares minimization of (19) to recover the angles φ^r_1 and φ^r_2 corresponding to the input angles φ^i_1 and φ^i_2; the latter were both allowed to vary over 360° in steps of 25°. The error $\Delta\varphi_{1,2} = \varphi^r_{1,2} - \varphi^i_{1,2}$ was formed, and its rms value calculated for all input angles. The result for the measured patterns used is $\sigma_{\Delta\varphi} = 34.8°$.

It is not surprising that patterns distorted as badly as those shown here will produce significant errors if they are not accounted for; 35° is too large an error in bearing to tolerate in

ocean surface measurements. Hence, the development and use of the methods in this paper to eliminate such errors are necessary and justified.

IV. Discussion and Conclusions

Distortion of the individual patterns of CODAR antenna elements can occur in many applications. It is desirable to avoid such distortion when possible, but when it is not, one should attempt to understand and deal with it. Two types of distortion should be differentiated; near-field and far-field distortion. The latter arises when obstacles are placed more than two wavelengths from the antenna system. In this case, the far-field radiated signals are partially reflected and blocked by the object, but in the same way for all three antennas. Such distortion is represented as a common multiplicative pattern factor occurring identically in the voltage integrals, (1), for all three antenna elements. It can then be considered to be absorbed in the common factor $g(\varphi)$ (as we illustrated subsequently), *and the remaining analysis* (for currents, waves, and transponder tracking) *done as though the antenna patterns were perfect,* i.e., using the methods of [3]. Situations where this happens include operation from shore in the vicinity of a pier. Also, bearings nearly tangent to the coastline have greater signal attenuation than those straight out from shore, appearing therefore as a pattern cutback for all three elements. In other words, this type of far-field distortion can be ignored for current, wave, and transponder drift measurements and the prior perfect-pattern methods can be used with no error.

Near-field distortion must be measured and dealt with in the extraction methods. One such method was presented and demonstrated in this paper. Near-field distortion is produced by metallic objects unsymmetrically placed within one wavelength of the antenna system. In this case, the obstacle actually becomes part of the antenna structure itself, much like the unfed director of a Yagi–Uda array. Such distortion will affect each element pattern in a different fashion, and hence cannot be divided out. An example of this type of distortion is calculated and shown in Fig. 1 for a loop–monopole system with a vertical off-center rod below it. In normal CODAR applications, we have found that this contamination can be expected for operations from metal offshore platforms, even when the antenna system is placed at the very top of the derrick or tower. *Neglect* of the distortion in the extraction methods will produce 35° rms errors in bearing extraction, based on actual patterns measured from platforms. Hence, special methods for dealing with such distortion must be implemented. We have never encountered pattern distortion of this type in coastal CODAR operations with the crossed-loop system, as long as care is taken to isolate feeder lines near the antenna using baluns. (We have always measured patterns during coastal operations to verify this claim.) On the other hand, the older four-element CODAR monopole array exhibits this type of differential pattern distortion due to mutual coupling among elements [5]; this type of pattern distortion is known to contribute bearing biases in current maps when uncorrected [9]. Mutual coupling does not occur with the crossed-loop/monopole system because of the physical and electrical orthogonality among the elements.

Not mentioned specifically in this paper are other supporting but secondary calibrations and steps that were discussed in detail in [3]. For example, it is assumed that amplitude and phase corrections among the three element signals (that may change as a function of time due to hardware drifts) are measured regularly and applied in the software. Methods very similar to those described in [3], based on the sea echo signal, are applied when the patterns are distorted also. It is assumed that although the amplitudes and phases may drift, the individual patterns do *not* change once the antenna and its near-field environment are fixed. Finally, the covariance matrix among the cross spectra used in the least-squares formulation is required (as in [3]) for the optimal extraction of current vectors and their statistical uncertainties. This is readily obtained using the techniques given in [3, appendix B] to arrive at a matrix analogous to [3, eq. (18)].

Acknowledgment

The authors are indebted to the careful measurements and instrumentation of the engineers and technicians of Codar Technology, Inc., to helpful discussions with Dr. M. W. Spillane of Gulf Oil Exploration and Development Company, and to SAGA Petroleum, A/S of Norway for their support.

References

[1] D. E. Barrick, M. W. Evans, and B. L. Weber, "Ocean surface currents mapped by radar," *Science,* vol. 198, pp. 138–144, 1977.

[2] T. M. Georges, Ed., "Coastal ocean dynamics applications radar: A user's guide," NOAA Wave Propagation Lab. Rep., Boulder, CO, Nov. 1984.

[3] B. J. Lipa and D. E. Barrick, "Least-squares methods for the extraction of surface currents from CODAR crossed-loop data: Application at ARSLOE," *IEEE J. Ocean. Eng.,* vol. OE-8, pp. 226–253, 1983.

[4] D. E. Barrick and B. J. Lipa, "A compact transportable HF radar system for directional coastal wavefield measurements," in *Ocean Wave Climate,* M. D. Earle and A. Malahoff, Eds. New York: Plenum, 1979, pp. 153–201.

[5] D. E. Barrick, "CODAR directional biases with a four-element antenna array," *IEEE Trans. Geosci. Remote Sensing,* vol. GE-24, no. 3, pp. 415–420, May 1986.

[6] S. T. Li, J. W. Rockway, J. C. Logan, and D. W. S. Tam, *Microcomputer Tools for Communications Engineering* (MININEC). Dedham, MA: Artech House, 1983, ch. 4.

[7] J. A. Leise, "The analysis and digital signal processing of NOAA's surface current mapping system," *IEEE J. Ocean. Eng.,* vol. OE-9, pp. 106–113, 1984.

[8] P. A. Miller, R. S. Lyons, and B. L. Weber, "A compact direction-finding antenna for HF remote sensing," *IEEE Trans. Geosci. Remote Sensing,* vol. GE-23, pp. 18–24, 1985.

[9] F. Schott, A. S. Frisch, K. Leaman, G. Samuels, and I. Popa Fotino, "High-frequency Doppler radar measurements of the Florida current in summer 1983," *J. Geophys. Res.,* vol. 90, no. C5, pp. 9006–9016, 1985.

★

Donald E. Barrick (M'62), for photograph and biography please see this issue, p. 146.

★

Belinda J. Lipa, for photograph and biography please see this issue, p. 245.